Characterization of LB thin films of a novel 2-(4-methoxyphenylamino)-2-oxoethyl methacrylate and sensing properties towards volatile organic vapors

Y. Acikbas[a,*], N. Cankaya[b], R. Capan[c], M. Erdogan[c], C. Soykan[a]
[a] Department of Materials Science and Nanotechnology Engineering, Faculty of Engineering, University of Usak, 64200 USAK/TURKEY
[b] Department of Chemistry, Faculty of Science, University of Usak, 64200 USAK/TURKEY
[c]Department of Physics, Faculty of Science, University of Balıkesir, 10145 BALİKESİR/TURKEY
yaser.acikbas@usak.edu.tr

Abstract: The synthesis, characterization and vapor sensing applications of a novel 2-(4-methoxyphenylamino)-2-oxoethyl methacrylate (MPAEMA) materials are reported in this study. FT-IR, ^{1}H and ^{13}C NMR spectra are used to analayze the structure of novel MPAEMA monomers. The thin film deposition conditions of MPAEMA monomer materials, which are prepared by LB film technique, are characterized by UV-vis spectroscopy and Quartz Crystal Microbalance (QCM) techniques. Transfer ratio values are found to be over 92 % for different substrates. The typical frequency shift per layer is obtained as 20.30 Hz / layer and the deposited mass onto a quartz crystal is calculated as 763.54 ng / layer. Vapor sensing properties of these LB films against five different volatile organic compounds are studied using the QCM technique. The sensitivities to vapors are determined between 6.82×10^{-4} and 1.63×10^{-4} Hz ppm^{-1}. MPAEMA LB film is more sensitive to chloroform and dichloromethane than other vapors. Responses of the MPAEMA LB film to these vapors are fast, large and reversible. Detection limits are calculated between 0.43×10^{4} and 1.84×10^{4} ppm. It can be concluded that this novel MPAEMA material is promising as a vapor sensing device at room temperature.

Key-Words: Monomer; Vapor sensor; Quartz crystal microbalance; LB thin film; Gas sensor.

1 Introduction

Methacrylate monomers/polymers are among the most important commercial polymers with a wide range of applications. They are used in products as diverse as glazing, lighting housings, bath tubs and structural adhesives. The success of these polymers in many of the applications is dependent on the versatility of the acrylic monomers in copolymerizing to produce a wide diversity of structures, which can be tailored to produce the desired properties. In recent years, special attention has been dedicated to polymers based on aminomethacrylates, since the presence of amine groups in the monomers eliminates the amino functionalization step, necessary to introduce amine-functional groups in the polymer [1]. Different aminomethacrylate monomers are used for the synthesis of polymeric membranes and chromatographic supports suitable for retention and separation in different fields such as waste water purification, solid phase extraction, protein recovery and purification, drug delivery systems and biochemical sensors among others [2, 3].

Monomeric/polymeric materials are also used as environmentally responsive coatings in volatile organic compounds (VOCs) detection due to their ability to absorb a variety of different molecules. VOCs such as chloroform, dichloromethane, acetone, benzene, toluene, ethyl alcohol, xylene and hexane are a large group of air pollutants. The majority of VOCs found in the indoor environments originate from building materials, indoor furnishings, cleaning supplies, consumer products and processes, such as printing, cooking, cleaning and pesticide applications [4, 5]. The effects of VOCs exposure depends on several parameters including the type of VOCs, the amount of VOCs and the length of time a person is exposed. High concentration exposure to some VOCs over a short or long term may cause diseases or serious irreversible effect [6, 7]. The detection of VOCs is one of the most important issue for the protection of human health and environment. In recent years, a significant interest in chemical sensing applications of organic materials such as carbon nanotubes [8], porphyrins [9], phthalocyanines [10], perylenes (PDIs) [11], indane [12], calix[n]arene [13] and

ISBN: 978-1-61804-306-1

polymers [14] are studied in order to fabricate a highly sensitive, easy to use, cheap, selective and a long life sensor. When a material interacts with VOCs, physical, chemical or structural properties have a change, either reversibly or irreversibly, i.e., color, mass, conductivity, film thickness, refractive index etc. The most important process in VOCs identification is the preparation of thin film sensors. There are many methods for thin film fabrication such as casting, spin coating, chemical or physical vapor deposition, and Langmuir-Blodgett (LB) thin film technique. Using LB technique, compared with other coating methods, it is possible to prepare a thin film with a controlled thickness at the molecular level with a well-defined moleculer orientation [15]. This technique can offer an effective way to prepare well defined structure of monomeric/polymeric LB film [16], which is promising for chemical sensors device application [17]. Fan et al. developed polymer and copolymer-coated Quartz Crsytal Microbalance (QCM) sensors for investigation of sensitive and selective detection of trace p-xylene [18] and 1-butanol vapors [19] in air. Fu and Finklea compared QCM sensors coated with molecularly imprinted polymers with nonimprinted polymers in terms of sensitivity and selectivity toward organic vapors [20]. The study demonstrated that imprinted polymers exhibit greater sensitivity and higher selectivity than the nonimprinted ones towards organic vapors (toluene, benzene, trichloroethylene, carbon tetrachloride and heptanes). A study used a QCM sensor coated with β-cyclodextrinpolymer thin film for the detection of benzene, toluene, and p-xylene at low concentrations and p-xylene showed the highest detection sensitivity [21]. Similar works were performed using the paraoxon imprinted polymer as sensing materials for real time paraoxon detection using QCM technique [22].

Our present study describes a synthesis, characterization and sensing application of a novel 2-(4-methoxyphenylamino)-2-oxoethyl methacrylate (MPAEMA) material. FTIR, ^{1}H-NMR and ^{13}C-NMR results are used to monitor the synthesis process of MPAEMA molecule. UV-vis and QCM methods are employed to demonstrate the thin film deposition onto the quartz glass or quartz crystal substrate. QCM method is also used to record the response of the sensor properties of MPAEMA LB films towards the following organic vapors: chloroform, dichloromethane, acetone, benzene and toluene.

2 Experimental Details

2.1. Synthesis of 2-(4-methoxyphenylamino)-2-oxoethyl methacrylate

Triethylamine (NR_3), 4-methoxyaniline, sodium methacrylate, and chloroacetyl chloride, (Aldrich) were used as received. Triethylbenzylammoniumchloride (TEBAC) as a phase transfer catalyst and distilled under vacuum (bp: 162 ^{o}C at 5 mmHg) (Aldrich). Acetone and 1,4 dioxane solutions were dried on anhydrous $MgSO_4$ and freshly distilled prior to use. 2-chloro-N-(4-methoxyphenyl)acetamide was synthesized similar to literature [23]. 4-methoxy aniline and NR_3 were dissolved in 100 ml acetone at 0–5 ^{o}C, and then chloroacetyl chloride was added drop wise to the solution. The reaction mixture was stirred at room temperature for 15 h. The precipitate was filtered off, a little of acetone removed by a rotary evaporator, the reaction mixture was crystallized from ice-water mixture. A shine lilac powder product was obtained (yield 80 %). The reaction scheme is shown in Fig. 1a. 2-chloro-N-(4-methoxyphenyl)acetamide (1 mol), sodium methacrylate (1.2 mol) TEBAC and NaI as catalyst were stirred in 50 ml 1,4 dioxane at 85 ^{o}C in a reflux condenser for 30 h in the presence of 100 ppm hydroquinone as inhibitor. Then the solution was cooled to room temperature and neutralized with a 5 % NaOH solution. The organic layer was washed several times with water and the water layer was washed with diethyl ether a few times. After, dried over anhydrous $MgSO_4$ overnight, diethyl ether was evaporated, and thus methacrylate monomer is given (yield 75 %). Synthesis of monomer is indicated in Fig. 1b [24, 25].

(a)

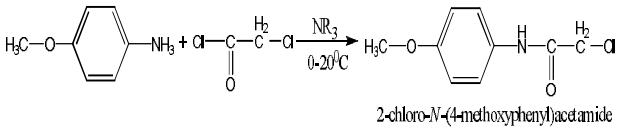

2-chloro-*N*-(4-methoxyphenyl)acetamide

(b)

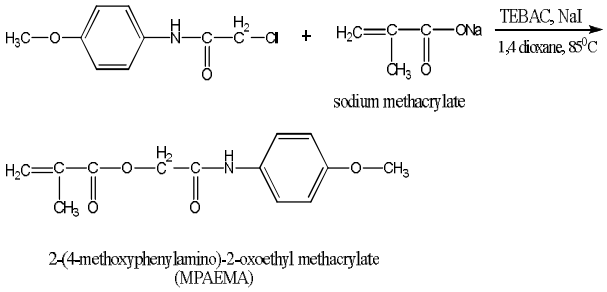

Fig. 1. (a) Synthesis of the 2-chloro-N-(4-methoxyphenyl)acetamide (b) Synthesis of the MPAEMA monomer.

2.2. Fabrication of MPAEMA LB thin film

MPAEMA ($C_{13}H_{15}NO_4$) was dissolved in chloroform with a ratio of concentration of 0.28 mg mL^{-1}. A Hamilton syringe was used to spread the solution onto the pure water surface. A NIMA 622 type LB trough provided with a filter paper Wilhemly balance was employed to take an isotherm and to prepare an LB thin film. A time period of 15 min was allowed for the solvent to evaporate before the area enclosed by the barriers was reduced. The Π-A isotherm graphs of the MPAEMA were recorded to determine the deposition surface pressure value which was held constant during the transfer of the monolayers from the water surface onto solid substrates at pH 6.0. The isotherms were recorded with the compression speed of 200 cm^2 min^{-1}. The isotherm graph was repeated several times and the results were found to be reproducible. LB film monolayers were transferred onto the quartz glass and quartz crystal at a constant surface pressure of 14 mN m^{-1} at room temperature by the vertical dipping method. Transfer ratio values were found to be over 92 % for different substrates and all experimental data were taken at room temperature.

2.3. Deposition Process of MPAEMA LB thin film

The UV-vis spectra of LB film was recorded in the visible spectral region from 400 nm to 600 nm using an Ocean Optics UV-vis light source (DH-2000-BAL Deuterium Tungsten light source) and spectrometer (USB4000) in absorbance mode. MPAEMA material was dissolved in chloroform and a UV-vis spectra was measured as a reference in a quartz cuvette. After each deposition of LB film layer onto a quartz glass substrate, UV-vis spectra were recorded again. These two UV-vis spectra were used to check the deposition process of MPAEMA LB films. Similar investigation was carried out using QCM measurement system. Fig. 2 shows a block diagram of our home made QCM measurement system. A thinly cut wafer of raw quartz sandwiched between two electrodes in an overlapping keyhole design was used for the QCM measurement. AT-cut quartz crystals with a resonant frequency of 3.5 MHz were commercialized from GTE SYLVANIA company. All measurements were taken at room temperature (23 ^oC) using an oscillating circuit. At the beginning of the measurement, a clean quartz crystal was inserted into the electronic unit, and the quartz crystal was placed in a gas chamber. In order to obtain f_0, which is the resonant frequency of non-coated quartz crystal, the frequency shift of quartz crystal was measured, and the frequency response was stable within ± 1 Hz over a period of 30-45 min. After each deposition cycle, the LB film sample was dried for half an hour and the mass change was monitored using this computer controlled QCM measurement system. This system was used for the confirmation of the reproducibility of LB film multilayers using the relationship between the QCM frequency changes against the deposited mass, which should depend on the number of layers in the LB film.

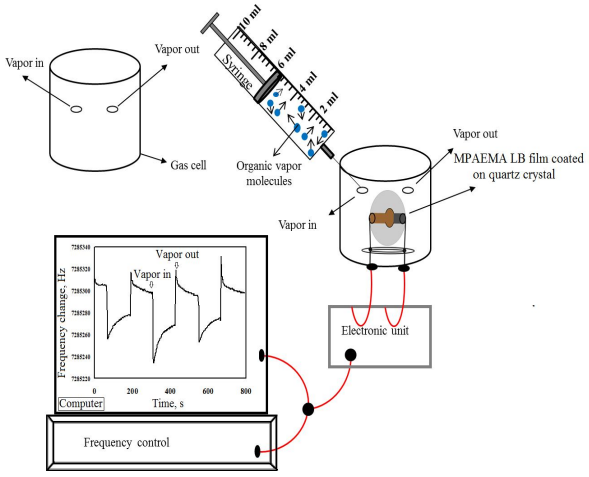

Fig. 2. A block diagram of the quartz crystal microbalance measurement system.

QCM measurement system was also employed to study the kinetic response of the LB sample against different organic vapors. A gas cell was constructed

to study the LB film response on exposure to organic vapors by measuring the frequency change and these measurements were performed with a syringe. The sample was periodically exposed to organic vapors at least for 2 min, and was then allowed to recover after injection of dry air. The changes in resonance frequency were recorded in real time during exposure to organic vapors. During this procedure the volume of VOC vapor introduced into the gas cell varied between 2-10 ml. The exposure to VOC vapor for 2 min was followed by flushing of the cell with dry air for another 2 min. This procedure was carried out over several cycles to observe the reproducibility of the LB film sensing element.

3 Results and Discussion

3.1. Characterization of MPAEMA monomer

FTIR spectra were obtained with a Perkin Elmer Spectrum One FTIR spectrophotometer on solid samples as KBr pellets. NMR spectra were recorded on a Bruker 400 MHz spectrometer at room temperature in DMSO-d_6.

FTIR, ^{1}H and ^{13}C NMR spectrums of monomer are indicated in Fig. 3, Fig. 4 and Fig. 5, respectively.

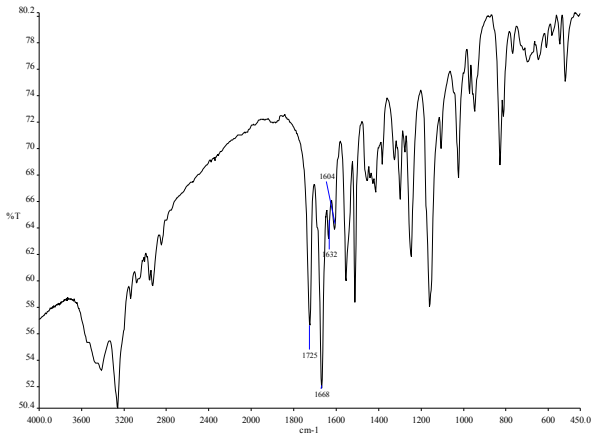

Fig. 3. FTIR spectrum of the MPAEMA monomer.

IR (cm^{-1}, the most characteristic bands): 1632 (C=C olefinic stretch), 1668 (C=O amide stretch), 1725 (C=O stretch), 1604 (C=C ester stretch on aromatic ring). ^{1}H-NMR spectrum of monomer following peaks appear; at 9.9 ppm for N-H, 7.3 and 6.7 ppm for aromatic ring protons, 5.9 and 5.6 ppm for =CH olefinic protons, 4.6 ppm O-CH_2, 3.6 ppm O-CH_3, 1.8 ppm for C-CH_3 protons. ^{13}C-NMR spectrum of monomer following peaks appear; at 166 ppm for amide C=O, 165 ppm for ester C=O, 135 ppm for CH_3-C=, 155, 132, 121 and 114 ppm for aromatic ring carbons, 127 ppm for =CH olefinic, 63 ppm for O=C-CH_2-O, 55 ppm O-CH_3, 18 ppm for C-CH_3 carbons.

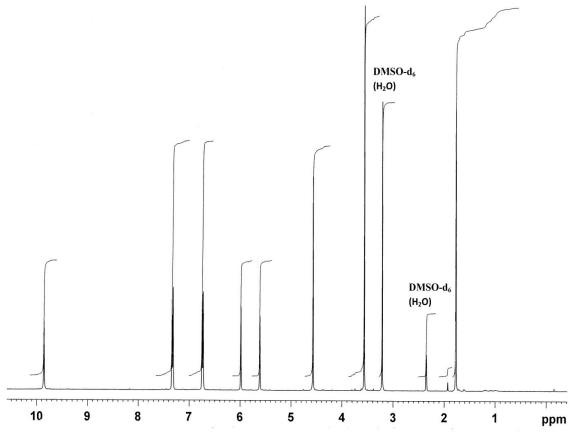

Fig. 4. ^{1}H-NMR spectrum of the MPAEMA monomer.

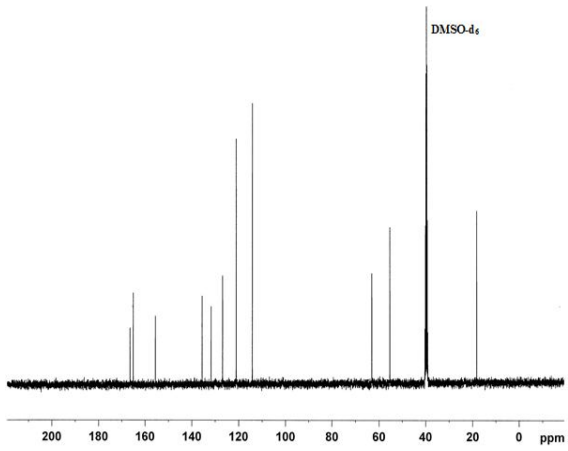

Fig. 5. ^{13}C-NMR spectrum of the MPAEMA monomer.

3.2 Isotherm and transfer ratio

The surface pressure versus surface area (Π-A graph) is an important graph to understand the characteristic surface behaviour of a floating monolayer on the water surface. The area per molecule for a floating monolayer can be calculated using this following relation:

$$a_m = AM_w / cN_A V \qquad (1)$$

where, A is the area of the water surface enclosed by the trough barriers, M_w is the molecular weight, c is the concentration of the spreading solution, N_A is the Avagadro's number, and V is the volume of solution spread over the water surface. The Π-A graph for MPAEMA monolayer at pH 6 is shown in Fig. 6. Using this graph and Eq.1 the limiting area per molecule can be obtained by extrapolating the slope of low compressibility to zero pressure and indicates 0.0814 nm^2 for V=900 µl and 0.0812 nm^2 for V=1200 µl. Similar results were observed for the behaviour of CODA (A coumarin-substi tuted diacetylene monomer) and BNADA (Bisazobenzene-substituted diacetylene monomer) monolayers at the air-water interface. The values of the limited molecular area, extrapolated from the linear portion of the Π-A isotherm to the zero surface pressure, are found to be about 0.19 nm^2 [26] and 0.21 nm^2 [27] for CODA and BNADA, respectively. The spreading behaviour of *N-N'*-dialkylacrylamide (dAAs) monomers on a water surface is investigated by measurement of surface pressure-area isotherms as a function of alkyl chain length and temperature. The isotherms show that the properties of the monolayers change definitely with the alkyl chain lengths and temperature. Miyashita et al. observed that the variation of temperature and alkyl chain length exerts the same effect on the behaviour of dAAs monolayers on the water using the limiting area per molecule parameter [28]. Collapse is not observed for MPAEMA monolayers where the order of monolayer is destroyed. Our results for MPAEMA material indicate good stability and reproducibility of the monolayers at the water surface.

The surface pressure value of 14 mN m^{-1} was selected as the fabrication pressure value in this study. Floating monolayers at the air-water interface were deposited onto the solid substrate on both upward and downward through the subphase. Similar value (22 mN m^{-1}) was chosen for three novel azobenzene-substituted diacetylene monomers (DA1, DA2 and DA3) monolayers formed on a water surface could be transferred onto solid substrates [29].

The transfer ratio given in Eq. 2 is an important parameter used to check the deposition of LB layer. This parameter is defined as the ratio of the area of the LB film removed from the water surface to the area of the substrate moved through the air-monolayer-water interface.

$$\tau = A_L / A_S \qquad (2)$$

where, A_L is the decrease in the area occupied by the monolayer on the water surface, and A_S is the coated area of the substrate.

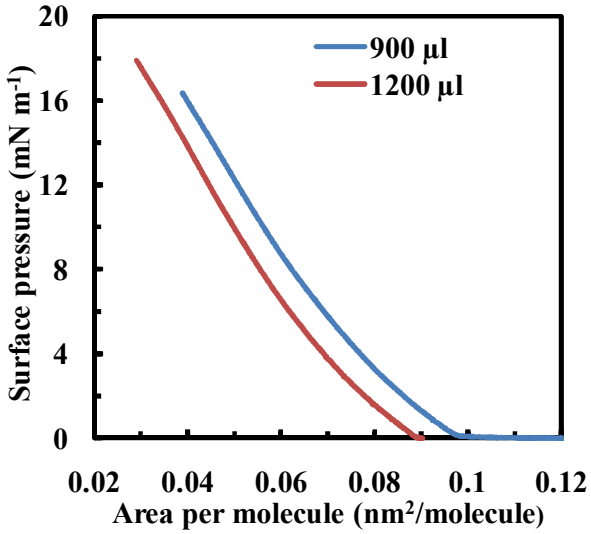

Fig. 6. Isotherm graphs of MPAEMA monolayer.

The MPAEMA monolayer during the deposition onto a quartz crystal substrate for 2 bilayers is given in Fig. 7. It is found that the average reduction of the area for each bilayer was almost the same during the deposition process of monolayers onto quartz crystal substrate. Using Eq. 2 transfer ratio values are calculated to be ≥ 92 % for a quartz glass and ≥ 96 % for a quartz crystal substrate. With these results it can be concluded that uniform Y-type MPAEMA LB films were deposited onto both substrates. Similar result is observed in study on the octadecyl trimethyl ammonium bromide (OTAB), which transfer ratio was found to be 98 % [30]. These results indicate that uniform and reproducible LB deposition is achieved.

ISBN: 978-1-61804-306-1

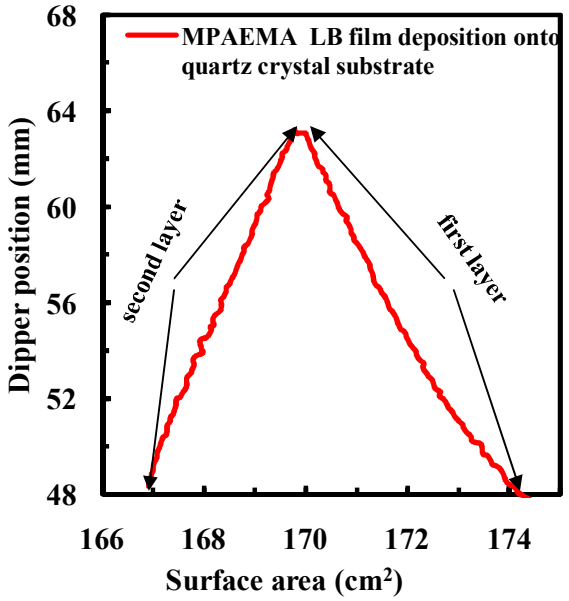

Fig. 7. The deposition graphs of MPAEMA LB film on the quartz crystal.

3.3. QCM measurements

QCM system is used for measuring the resonance frequency of quartz crystal between electrodes which is fairly sensitive to a small mass change at a nanoscale. This measurement technique was first described by Sauerbrey and the resonance frequency change (Δf) on LB film multilayer quartz crystal against a mass change per unit area (Δm) is given by [31]:

$$\Delta f = -\left(2 f_0^2 \Delta m / \rho_q^{1/2} \mu_q^{1/2} A\right) N \quad (3)$$

where, N is the number of deposited LB film layers, Δm is the deposited mass per unit area per layer (g), Δf is the frequency change (Hz), f_0 is the resonant frequency of non-coated quartz crystal (Hz), A is the electrode active area (2.65 cm^2), ρ_q is the density of quartz (2.648 g cm^{-3}) and μ_q is the shear modulus of quartz (2.947x 10^{11} g cm^{-1} s^{-2}).

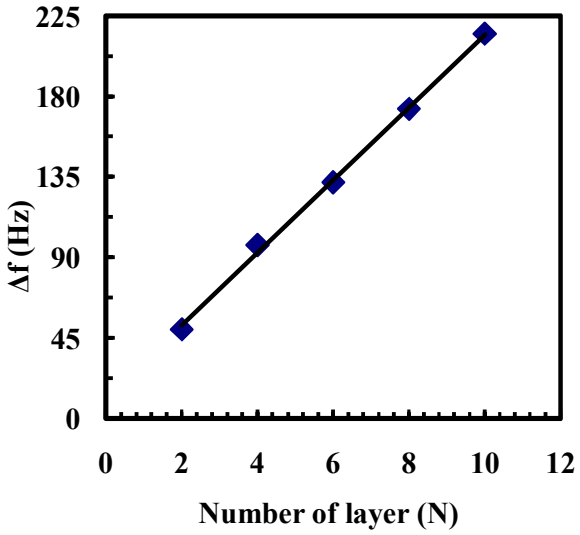

Fig. 8. Frequency changes as a function of MPAEMA LB film layer numbers.

Fig. 8 shows the relationship between frequency difference and number of layer during the transfer process of MPAEMA LB films onto quartz resonators. A systematic change in resonance frequency with the increase in the number of monolayers is clearly observed. This change described Eq. 3 is closely associated with the mass change of LB layers on the substrate and is highly reproducible and uniform. It also suggests that equal mass per unit area is deposited onto the quartz crystal during the transfer of LB film layers. Typical frequency shift of 20.30 Hz / per layer for MPAEMA LB film is obtained from the slope of the plot. The mass deposited on the quartz crystal per bilayer is estimated as 763.54 ng (2.88 ng mm^{-2}) for MPAEMA LB film using Eq. 3 and Fig. 8.

3.4. UV-visible results

Fig. 9 displays UV-vis absorption spectra of a MPAEMA solution in chloroform and MPAEMA LB films transferred onto a quartz substrate with different layer. A peak for MPAEMA solution is observed at around 225 nm and this peak is shifted to 250 nm when LB film is deposited to quartz glass substrate. The absorption intensity increased when the number of layers increased. Both spectra are similar except that the bands at 225 nm is broadened in the solution spectrum and is red shifted by about 25 nm. This shift in the absorption band of the LB film may be the result of some kind of molecular aggregation which takes place during film

ISBN: 978-1-61804-306-1

formation. It has been attributed to two possible reasons such as an edge-to-edge aggregation of the MPAEMA molecules in the monolayer film and the conformational change of the MPAEMA macrocycle from nonplanar structures in solution to planar structures in solid films. When comparing the limiting molecular area of the MPAEMA monolayer on the water surface, it is unlikely that the MPAEMA molecules formed edge-to-edge aggregation within the monolayer film. It is more reasonable to attribute the red shift of the main absorption bands to a greater π-electron delocalization in the film than in solution because of the more planar conformation of the macrocycle in the film. Similar results are observed for CDM (the monomer material) solution and the 16-layer CDM LB film [32].

In order to monitor the deposition of MPAEMA LB film layer onto the quartz substrate, the relationship between the absorbance and mass deposition is investigated. The inset in Fig. 9 shows variations of absorption intensity at 250 nm as a function of number of layers. This linear relationship confirms a fairly constant mass ratio during sequential dipping of the slide through the LB monolayer. This demonstrates successful adhesion of the monolayers to the quartz glass substrate.

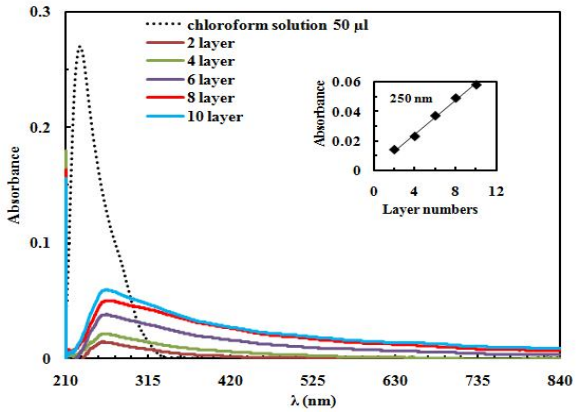

Fig. 9. UV-vis spectras of MPAEMA in a chloroform solution and MPAEMA LB film on the quartz. Inset: linear increase of absorbance as a function of layer numbers.

3.5 Sensing properties of MPAEMA LB film

In order to study the potential application of this MPAEMA LB film in the field of VOCs sensing, the kinetic response of the LB sample to chloroform, dichloromethane, acetone, benzene and toluene vapors is recorded by measuring the resonance frequency as a function of time. The LB film sample is periodically exposed to the organic vapor for 2 min, followed by the injection of dry air for a further 2 min period. Fig. 10 shows the kinetic response of the MPAEMA LB film to the vapors. This LB film shows a response to all vapors with a fast, reproducible and reversible response after flushing the gas cell with fresh air. The frequency change (Δf), response and recovery times of MPAEMA LB film against organic vapors were presented in Table 1. The response of the LB film in the form of QCM responses to saturated chloroform and dichloromethane exposures are much higher than the other vapors with recovery and response times in the order of a few seconds when the gas cell is flushed with dry air.

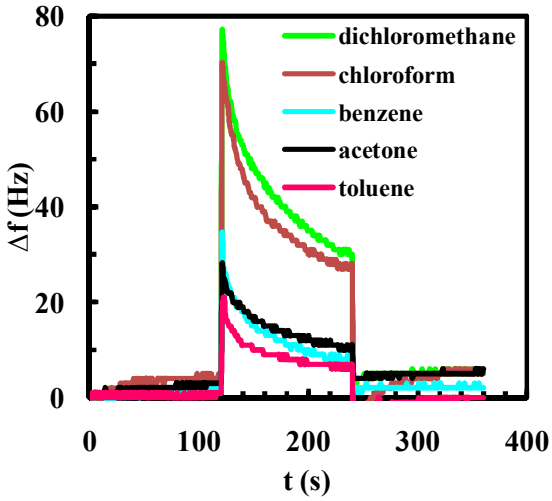

Fig. 10. The frequency change of MPAEMA LB film against organic vapors.

Table 1. The frequency change, response and recovery times of MPAEMA LB film against organic vapors.

Organic vapors	Response time (s)	Recovery time (s)	Δf (Hz)
Chloroform	4.2	4.5	77
Dichloromethane	4.1	4.3	70
Benzene	3.2	3.5	34
Acetone	3.4	3.1	28
Toluene	2.2	3.2	21

ISBN: 978-1-61804-306-1

In general, the mechanism of gas permeation into the sensing material can be considered by three "solution-diffusion" steps, i.e., adsorption, diffusion, and desorption process. In the first step, the frequency decreases sharply until reaching a stable value at the time when initial influence occurs between LB film sensor and vapor, which is due to surface adsorption [33]. In the second step is a diffusion process which vapor molecules penetrate into the LB film sensor. The interaction of LB films with the adsorbed vapors is a dynamic process where adsorption and desorption processes occur simultaneously when the sensor is exposed to vapors. The resonance frequency reaches a stable state after dynamic balance where the number of adsorbed vapor molecules is equal to the number of desorbed vapor molecules. In the last step, the sensor is exposed to fresh air and the resonance frequency increases due to desorption of vapor from the surface of the sensor. The inset Fig. 11 shows the real-time response of the MPAEMA LB film sensor to different volumes of chloroform. The initial step is to present dry air to obtain a baseline. Then, the sensor is exposed to a certain volume of chloroform gas (2.98 x 10^4-14.94 x 10^4 ppm), which leads to a frequency shift until a steady-state is reached. When the sensor is exposed to chloroform gas, the frequency shift initially increases rapidly and then reaches a point of stability. It is obvious that the frequency shift increases when the volume of chloroform is increased.

In Fig. 11 the kinetic gas response of the MPAEMA thin film in exposure to different volumes of VOCs vapors is given in terms of the change in resonance frequency (Δf) over time. The VOCs vapor was injected into the gas cell for 2 min at diluted amounts of saturated concentration followed by 2 min recovery with dry air. The concentrations of VOCs vapor (saturated gas diluted with dry air) used were 20 %, 40 %, 60 %, 80 % and 100 %. The Δf of the quartz crystal resonator increases with the introduction of VOC vapor into the gas cell where increasing the volume of VOC vapor leads to higher response as can easily be predicted.

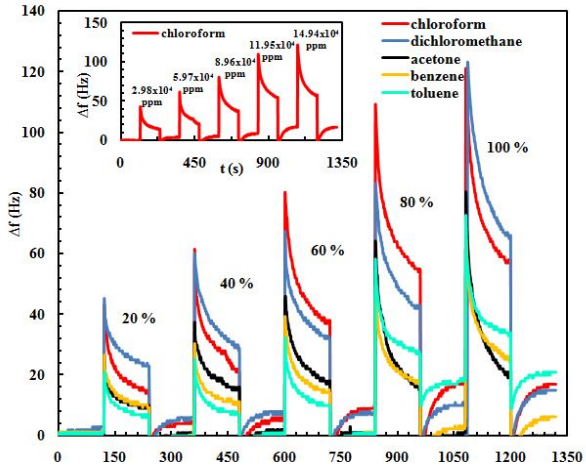

Fig. 11. The response of MPAEMA LB sensor to different concentrations. Inset: the response of MPAEMA LB sensor from 2.98 x 10^4 to 14.94 x 10^4 ppm of chloroform vapors.

The frequency shifts of MPAEMA LB thin film sensor versus the volumes of the five VOCs were plotted and shown in Fig. 12. After each injection of VOCs, the adsorption of VOCs onto the LB thin films resulted in a decrease in the resonance frequency of the quartz crystals. It was found that with the enhancement of gas volume, the frequency shift increases and gives an almost linear response to gas volume for chloroform, dichloromethane, acetone, benzene and toluene. The concentration values of organic vapor in ppm can be calculated by the following formula [18]:

$$c = \left[(\rho V / M) \text{x} 10^6 \right] / \left[V_0 / (24.055 L / mol) \right] \quad (3)$$

$$c = \left[24.055 \rho V / M V_0 \right] x 10^6 \quad (4)$$

where, c (ppm) is the concentration of VOC vapor, ρ (g/mL) is the density of VOC, V (mL) is the volume of VOC vapor which is injected into the gas chamber, M (g/mol) is the VOC molecular weight, and V_0 is the volume of the gas chamber (i.e. ~ 0.02 L). The vapor volume values used in this study are 20 % for V= 2 mL, 40 % for V= 4 mL, 60 % for V= 6 mL, 80 % for V= 8 mL, and 100 % for V= 10 mL.

The limit of detection (LOD) of the MPAEMA LB film sensor is calculated by the measured sensor sensitivity (Hz / ppm) which is given by [33]:

$$LOD = 3\sigma / S \quad (5)$$

where σ is the noise level of the fabricated QCM sensor; and S is the sensitivity to a specific analyte of the sensor.

The sensitivity of LB film sensor is obtained from the frequency shift curves when exposed to organic vapors in Fig. 12. The approximate values of the curves are obtained from this figure. The resonance frequency is recorded in air for use as the absolute frequency of the QCM system, and the frequency response is stable within ± 1 Hz over a period of 30-45 min. Therefore, the frequency noise is assumed at 1 Hz. The sensitivity and detection performance of the fabricated QCM sensor to several volatile organic vapors is given in Table 2. The MPAEMA-coated QCM sensor displayed sensitivity with detection limits of 0.43 x 10^4 and 1.84 x 10^4 ppm for various organic vapors at room temperature. The values of sensitivity are found as chloroform > dichloromethane > acetone > benzene > toluene, for MPAEMA materials (can be seen Table 2).

Table 2. Sensitivity of the MPAEMA-coated QCM sensor to different chemical vapors.

Organic vapors	Sensitivity (Hz / ppm) x 10^{-4}		Detection limit (ppm) x 10^4
Chloroform	6.82	4.5	77
Dichloromethane	5.19	4.3	70
Benzene	3.29	3.5	34
Acetone	2.37	3.1	28
Toluene	1.63	3.2	21

These results can be explained in terms of molar volume and moleculer weight of organic vapors. The molar volume of organic vapors order is given as dichloromethane (64.10 cm^3 mol^{-1}) < acetone (72.74 cm^3 mol^{-1}) < chloroform (80.50 cm^3 mol^{-1}) < benzene (86.36 cm^3 mol^{-1}) < toluene (107.00 cm^3 mol^{-1}). Dichloromethane has the lowest molar volume parameter and penetrates easily into MPAEMA LB films while toluene has the largest molar volume and has a slow penetration into the LB film structure. However, the sensitivity of MPAEMA against chloroform vapor larger than dichloromethane vapor. This can be explained taking into account molecular weights, the moleculer weight of chloroform (119.38 g mol^{-1}) larger than dichloromethane (84.93 g mol^{-1}). A larger molecular weight of vapor leads to higher sensitivity, which is in good agreement with the previous findings in the literature [34]. It is reasonable to assume that if the number of adsorbed molecules on an adsorbent is limited and identical for various adsorbents, a greater molar mass of adsorbent would certainly lead to a larger frequency shift [33].

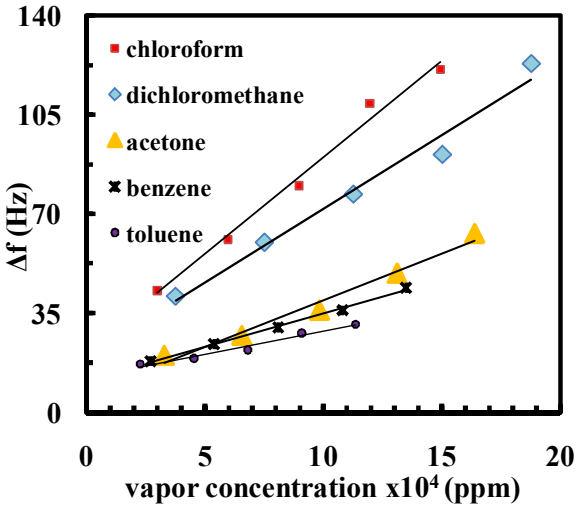

Fig. 12. Frequency shifts versus volumes of organic vapors.

4 Conclusions

In this study, the synthesis, characterization and vapor sensing properties of a novel 2-(4-methoxyphenylamino)-2-oxoethyl methacrylate (MPAEMA) materials were investigated using FT-IR, ^1H and ^{13}C NMR, UV-vis spectroscopy and QCM techniques. Isotherm graph demonstrated that the area per molecule for MPAEMA monolayer at the air-water interface was found to be approximately 0.082 nm^2 and a uniform LB deposition occured onto substrates. A plot of UV-vis absorbance value at 250 nm as a function of number of layers indicated a linear relationship. Similar linear relationship was obtained for resonant frequencies versus number of layer using QCM measurement. The typical Δf per layer is obtained as 20.30 Hz / layer and the deposited mass onto quartz crystal is calculated as 763.54 ng / layer (2.88 ng mm^{-2}). MPAEMA LB film was exposed to chloroform, dichloromethane, acetone, benzene and toluene vapors. The kinetic measurement of this LB film shows fast, reproducible and reversible response to all vapors. The sensitivities of the MPAEMA LB film sensor against organic vapors were obtained between 6.82 x 10^{-4} and 1.63 x 10^{-4} Hz ppm^{-1}. Detection limits were found to be

ISBN: 978-1-61804-306-1

between 0.43 x 10^4 and 1.84 x 10^4 ppm for various organic vapors. It can be proposed that the sensing element deposited onto quartz crystal substrate has good sensitivity and selectivity to chloroform and dichloromethane vapors. As a result, this MPAEMA material can be used as a sensing material and may find potential applications in the development of room temperature organic vapor sensing devices.

References:

[1] C. Soykan, F. Yakuphanoğlu, M. Şahin**,** *J. Macromol. Sci. A*, 50, 2013, 953-965.

[2] S. Barral, A. Guerreiro, M. A. Villa-García, M. Rendueles, M. Díaz, et al., *React. Funct. Polym.*, 70, 2010, 890-899.

[3] J.M. Cervantes-Uc, J.V. Cauich-Rodriguez, W.A. Herrera-Kao, H. Vázquez-Torres, A. Marcos-Fernández, *Polym. Degrad. Stabil.,* 93, 2008, 1891-1900.

[4] J.E. Colman Lerner, E.Y. Sanchez, J.E. Sambeth, A.A. Porta, *Atmos. Environ.,* 55, 2012, 440-447.

[5] Y. M. Kim, S. Harrad, R. M. Harrison, *Environ. Sci. Technol.*, *35,* 2001, 997-1004.

[6] J. Zhou, Y. You, Z. Bai, Y. Hu, J. Zhang, et al., *Sci. Total Environ.,* 409,2011, 452-459.

[7] S. C. Sofuoglu, G. Aslan, F. Inal, A. Sofuoglu, Int. *J. Hyg. Environ. Health*, 214,2011, 36-46.

[8] M. Consales, S. Campopiano, A. Cutolo, M. Penza, P. Aversa, et al., *Sens. Actuators B*, 118, 2006, 232-242.

[9] D. Çaycı, S.G. Stanciu, İ. Çapan, M. Erdoğan, B. Guner, et al., *Sens. Actuators B*, 158, 2011, 62-68.

[10] Y. Açıkbaş, M. Evyapan, T. Ceyhan, R. Çapan, Ö. Bekaroğlu, *Sens. Actuators B*, 135, 2009, 426-429.

[11] Y. Acikbas, R. Capan, M. Erdogan, F. Yukruk, *Sens. Actuators B,* 160, 2011, 65-71.

[12] M. Evyapan, R. Çapan, H. Namlı, O. Turhan, *Sens. Actuators B*, 128, 2008, 622-627.

[13] R. Capan, Z. Ozbek, H. Goktas, S. Sen, F.G. Ince, et al., *Sens. Actuators B,* 148, 2010, 358-365.

[14] M. Maute, S. Raible, F.E. Prins, D.P. Kern, H. Ulmer, et al., *Sens. Actuators B*, 58, 1999, 505-511.

[15] I. Capan, C. Tarımcı, R. Capan, *Sens. Actuators B,* 144, 2010, 126-130.

[16] A. Chyla, S. Kucharski, R. Janik, J. Sworakowski, M. Bienfikowski, *Thin Solid Films*, 284-285, 1996, 496-499.

[17] M. Zhong, Y. Teng, S. Pang, L. Yan, X. Kan, *Biosens. Bioelectron.*, 64, 2015, 212-218.

[18] X. Fan, B. Du, *Sens. Actuators B*, 166-167, 2012, 753-760.

[19] X. Fan, B. Du, *Sens. Actuators B,* 160, 2011, 724-729.

[20] Y. Fu and H. O. Finklea, *Anal. Chem.*, 75, 2003, 5387-5393.

[21] J. F. Ju, M.J. Syu, H. S. Teng, S. K. Chou, Y. S Chang, *Sens. Actuators B*, 132, 2008, 319-326.

[22] E. B. Özkütük, S. E. Diltemiz, E. Özalp, R. Say, A. Ersöz, *Mater. Sci. Eng. C*, 33, 2013, 938-942.

[23] F. Karatas, A. Cansiz, H. Kara, M. Karatepe, M. Koparir, Russ. *J. Bioorg. Chem.,* 31(5), 2005, 499-501.

[24] N. Çankaya and K. Demirelli, *J. Chem. Soc. Pak.,* 33(6), 2011, 884-892.

[25] C. Soykan, A. Şahan, F. Yakuphanoğlu, *J. Macromol. Sci. A*, 48, 2011, 169-176.

[26] Y. Xu, J. Li, W. Hu, G. Zou, Q. Zhang, *J. Colloid Interface Sci.,* 400, 2013, 116-122.

[27] X. Pan, H. Jiang, Y. Wang, Z. Lei, G. Zou, et al*., J. Colloid Interface Sci.*, 354, 2011, 880-886.

[28] T. Miyashita, Y. Ito, *Thin Solid Films* 260,1995, 217-221.

[29] G. Zou, Y. Wang, Q. Zhang, H. Kohn, T. Manaka, et al., *Polym.,* 51, 2010, 2229-2235.

[30] S. A. Hussain, D. Dey, S. Chakraborty, D. Bhattacharjee, *J. Lumin.*, 131, 2011, 1655-1660.

[31] G. Sauerbrey, *Z. Phys.* 155, 1959, 206-222.

[32] A. Riul Jr., D.M. Taylor, C.A. Mills, P.J. Murphy, *Thin Solid Films,* 366, 2000, 249-254.

[33] P. Sun, Y. Jiang, G. Xie, J. Yu, X. Du, et al., *J. Appl. Polym. Sci.*, 116, 2010, 562-567.

[34] L.G. Xu, X. Hu, Y.T. Lim, V.S. Subramanian, *Thin Solid Films,* 417, 2002, 90-94.

Acknowledgements

The authors would like to thank The Research Foundation of Usak University (BAP) for financial support of this work. Project no.: 2014/MF014.